Earth and Planetary Science Letters, 84 (1987) 27–41
Elsevier Science Publishers B.V., Amsterdam – Printed in The Netherlands

[6]

Nd and Sr isotopic variations of Early Paleozoic oceans

Lisette S. Keto and Stein B. Jacobsen

Department of Earth and Planetary Sciences, Harvard University, Cambridge, MA 02138 (U.S.A.)

Received December 1, 1986; revised version received March 10, 1987

We report $^{143}Nd/^{144}Nd$ and $^{87}Sr/^{86}Sr$ isotopic data for Lower Paleozoic phosphatic brachiopod and conodont fossils. The data appear to represent the isotopic values of Early Paleozoic seawaters. We show that different paleoceanic water masses can be distinguished on the basis of their ϵ_{Nd} signatures. Two sides of what is classically considered one circulating Iapetus Ocean have different ϵ_{Nd} signatures from at least the Middle Cambrian until the Late Middle Ordovician. We infer two ocean basins between North America and Baltica separated by an island and/or shoal circulation barrier. Thus, it appears necessary to redefine the area of the Iapetus Ocean. The ϵ_{Nd} signature of the redefined smaller Iapetus Ocean ranges from -5 to -9 and the ϵ_{Nd} signature of the larger, coeval Panthalassa Ocean, including part of what was formerly called the Iapetus Ocean, ranges from -10 to -20. The first time that the ϵ_{Nd} values are identical in these two water masses is coincident with the onset of the Taconic Orogeny of North America. The paleogeographic geometry we infer from this work is consistent with paleogeographic reconstructions having the Baltica continent at very high latitudes in the Early/Middle Ordovician. The ϵ_{Nd} and faunal distribution support temperature-controlled conodont faunal provinciality. A rough mean age for exposed continental crust in the Early Paleozoic can be obtained from the average ϵ_{Nd} value of Early Paleozoic Oceans. The data suggest that the mean age of the crust as a function of time has remained essentially constant or even decreased during the past 500 Ma, and suggest substantial additions of new crust to the continents through the Phanerozoic.

1. Introduction

The major oceans of the world vary in their concentration and isotopic composition of Nd. Every major ocean water mass today is characterized by a distinctive $^{143}Nd/^{144}Nd$ isotopic signature [1–3]. The uniqueness of that isotopic signature is due to differences in the isotopic composition of the inputs to each ocean. The differences in $^{143}Nd/^{144}Nd$ among oceans are maintained by the short time scale for the cycling of Nd within oceans since the residence time of Nd is considerably shorter than interocean mixing times. Strontium, however, has a much longer residence time in seawater. Thus, $^{87}Sr/^{86}Sr$ isotopic ratios are identical everywhere in oceans today [4,5].

Changes through time in the $^{143}Nd/^{144}Nd$ of seawater at any specific location reflect not only changes in large scale ocean circulation patterns but also changes in the isotopic composition of the inputs to the oceans. These inputs include river waters, hydrothermal waters and diagenetic waters. River waters are the most important volumetric input to the oceans and the dominant source of oceanic Nd [6]. When the differences in $^{143}Nd/^{144}Nd$ ratios among the ocean water masses were found, it was initially thought that the flux of Nd from hydrothermal circulation through mid-ocean ridges might contribute significantly to these variations [1]. It now appears that the concentration of Nd in hydrothermal waters is too low to significantly affect $^{143}Nd/^{144}Nd$ in any ocean today [7]. The $^{87}Sr/^{86}Sr$ ratio of the oceans, however, is significantly affected by both hydrothermal and river water contributions of Sr [6,8,9].

The characteristic $^{143}Nd/^{144}Nd$ value of each ocean reflects the mixing of waters with variable $^{143}Nd/^{144}Nd$ ratios from many source terranes around that ocean basin; i.e. the $^{143}Nd/^{144}Nd$ value in an ocean water mass averages $^{143}Nd/^{144}Nd$ from a large area of exposed land. Thus, the $^{143}Nd/^{144}Nd$ of the oceans through time is useful for tracing the isotopic evolution of the surface of the continental crust. By coupling data on Nd and Sr in the oceans, it is possible to obtain both global and local information.

In this paper, we report $^{143}Nd/^{144}Nd$ and

0012-821X/87/$03.50

$^{87}Sr/^{86}Sr$ isotopic ratios of Paleozoic biophosphate fossils which appear to have recorded the isotopic values of Paleozoic seawater. Some of these results have been published in abstract form [10]. We use the $^{143}Nd/^{144}Nd$ data to show that different paleoceans can be distinguished on the basis of their Nd isotopic signatures.

2. Biophosphates as tracers for $\epsilon_{Nd}(T)$ of paleoseawater

The $^{143}Nd/^{144}Nd$ of marine authigenic minerals may be used to estimate $^{143}Nd/^{144}Nd$ of paleoseawater [11–13,19]. The sample types that have been used are phosphorites, biophosphates including fish teeth and conodonts, and Fe-Mn coatings on foraminifers, and metalliferous sediments.

Biophosphate samples are probably the best available material for obtaining $^{143}Nd/^{144}Nd$ in paleoseawaters. They are fossil skeletons which can be assigned to specific geological ages. Biophosphates therefore give much better age control than non-biogenic phosphorites. Relatively common biophosphatic skeletal material includes conodonts, inarticulate brachiopods, fish bones and teeth. The apatite that makes up these fossils has higher concentrations of REE than any other common marine sedimentary mineral. Phosphates and biophosphates have enrichments of REE concentrations relative to seawater of 5–6 orders of magnitude [11,14]. REE concentrations in foraminiferal Fe-Mn coatings are 2–3 orders of magnitude lower than phosphorites, and Nd concentrations in fossil carbonates are 2–5 orders of magnitude lower than in fossil phosphates [11,13]. Thus, the REE of carbonate fossils and their coatings may be more easily affected than phosphate minerals by later contamination or alteration. It is also better to use a well characterized phase that incorporates REE into its lattice like apatite, rather than rely upon poorly characterized coatings that are likely to be highly reactive.

Additionally, organic material in biophosphate skeletons changes color in a systematic fashion depending on temperature and duration of burial. The relationship of conodont color to diagenetic burial history is called the color alteration index (CAI) [15]. By examining the color or CAI of phosphatic fossil samples, it is possible to select the fossils which are least likely to have suffered exchange of Nd during high temperature diagenesis. Biophosphate samples with CAI of up to 5 (indicating burial temperatures up to 350 °C) seem to retain their original Nd signature from the time of deposition [11].

Because conodonts are found only in rocks of Triassic to Cambrian ages, and inarticulate brachiopods are rare in rocks younger than the Devonian, phosphatic fossils are not available everywhere. Therefore other authigenic materials like phosphorites and carbonates (or their coatings) must also be used. An advantage of carbonate minerals and fossils is that they are much more common than phosphorites or phosphatic fossils throughout the geologic record. Carbonates have extremely high concentrations of Sr and have been used to study $^{87}Sr/^{86}Sr$ as well as O and C isotopes in paleoseawater [4,5,16].

All of the sample types used to represent $^{143}Nd/^{144}Nd$ in paleoseawater have a common problem. It is not clear that their Nd is derived directly from contemporaneous seawater. However, the biophosphatic samples have the best-studied and clearest relationship to seawater. Nd concentrations in some shark's teeth and inarticulate brachiopods show that REE concentrations in apatitic parts of living animals are quite low and the increase in concentration must occur after the creatures' death [11]. Yet, because biophosphate samples seem to obtain their high REE concentrations while the organism is at or slightly below the seawater sediment interface [17], the $^{143}Nd/^{144}Nd$ values in well-preserved biophosphatic fossils are most likely the same as those in contemporaneous seawater. Their REE patterns appear to reflect those of contemporaneous seawater [17]. Fe-Mn coatings on foraminiferas do not have REE patterns similar to those of seawater [13]. Although not extensively studied, inorganic phosphorites are presumed to behave similarly to biogenic phosphates.

3. Samples

Descriptions and locations of our samples are given in Table 1 and Fig. 1. They are grouped as follows: European (EU), North American except Southeastern United States (NA) and Southeastern United States (SE). Four samples are conodonts, thirteen are inarticulate brachiopods and

TABLE 1

Biophosphatic fossil samples

Sample	Species	Formation	Location	Series	Stage or Zone
I. European					
IB26	*Lingula*	Wenlock Limestone	Dudley, England	Wenlock, Silurian	Homerian
JR8	Conodonts	Top of Furudal Lm.	Fjacka, Siljan, Sweden	Llandeilian, L/M Ordovician	e *Pygodus enserius Zone*
IB1	*Obolus apollinus*	Sandstone	Leningrad, U.S.S.R.	L Ordovician	–
IB6	Lingulid	Sandstone	U.S.S.R., near Poland	L Ordovician	–
IB7	*Ungulites obolus*	Sandstone	Pavlovsk, U.S.S.R.	M Cambrian	–
II. North American (except Southeastern U.S.)					
IB3	*Lingula cereata*	Medina Sandstone	Lockport, New York (U.S.A.)	Basal Silurian	Medinian
IB11	*Acrotretid discina*	Trenton Limestone	between Milheim and Centerhall, Pa. (U.S.A.)	M Ordovician	Trentonian
C14	Conodonts	Simpson Limestone	Arbuckle Mtns. (U.S.A.)	L/M Ordovician	Chazyan
IB22	Lingulid and carbonate	Upper Goodwin Unit of Pogonip Limestone	Eureka, Nev. (U.S.A.)	L Ordovician	Canadian
IB8	*Obolus radulus*	St. John's Group	Near St. John, N.B., Canada	U Cambrian	–
IB12	*Acrotretid physothela*	Steamboat Pass Shale	Steamboat Pass, Nev. (U.S.A.)	U Cambrian	*Dunderbergia* Zone
IB2	*Lingula ampla*	Potsdam Sandstone	St. Croix, Wisconsin (U.S.A.)	U Cambrian	Dresbachian
IB5	*Obolella dicellomas*	Sandstone	Eau Claire, Wisconsin (U.S.A.)	U/M Cambrian	probably Dresbachian
IB10	*Acrotretid prototreta*	Lower Pole Canyon Fm.	Current Gap, Nev. (U.S.A.)	M Cambrian	*Albertella* Zone
IB9	*Acrotretid hadrotreta*	Combined Metals Member of Pioche Shale	Pioche, Nev. (U.S.A.)	L Cambrian	*Bonnia-Olenellus* Zone
III. Southeastern United States					
JR5a	Conodonts	Holston Fm.	Thorn Hill, Tenn., west of Saltville fault (U.S.A.)	L/M Ordovician	*Nemagraptus gracilis* Zone
JR5b	Conodonts	Blockhouse Shale	Mosheim, Tenn., east of Saltville fault (U.S.A.)	L/M Ordovician	*Glyptograptus teretiusculus* Zone
IB4	*Lingulella arcuata*	Cap Mtn. Member of Riley Fm.	Lion Mtn., Burnet Quad., Texas (U.S.A.)	U Cambrian	Upper Dresbachian

one is a mixture of inarticulate brachiopods and carbonate fossils. These Early Cambrian to Middle Silurian samples all have CAI values that are $\leqslant 5$.

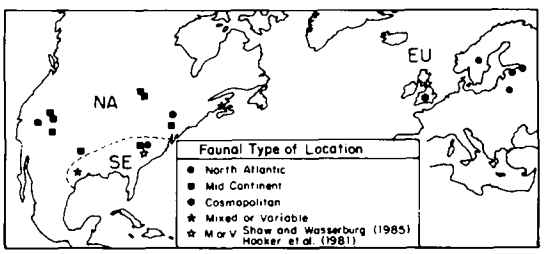

Fig. 1. Lower Paleozoic sample location map (including a phosphorite from Tennessee [11], and a metalliferous sediment from Scotland [19]). All samples are grouped as follows: by location: Europe (*EU*), North America except southeastern U.S. (*NA*), and southeastern United States (*SE*); by faunal type: North Atlantic (NAT), Mid-Continent (MC), Cosmopolitan (C), Mixed or Variable (MV). The Tennessee phosphorite [11] is a MV sample since it contains no fossils, and is from a region where either NAT or MC faunas can be found. A metalliferous sediment sample from an ophiolite sequence in Scotland [19] is another MV sample. Its location is near Girvan and appears to be part of the same allochthonous sequence. Girvan faunas contain Pacific brachiopods, and mixed Atlantic and Pacific trilobite [23,24].

At various times during the Early Paleozoic, biogeographic provincialism was exhibited by trilobites, brachiopods, graptolites and conodonts [20–23]. Since provincialism was most pronounced

TABLE 2

Analytical data for biophosphate samples

Sample	Location/ Fauna type [a]	$^{87}Sr/^{86}Sr$ [b]	Sm (ppm)	Nd (ppm)	$^{147}Sm/^{144}Nd$ [c]	$^{143}Nd/^{144}Nd$ [d]	$\epsilon_{Nd}(0)$ [e]
I. European							
IB26	England/C	-	578.2	2445	0.14155	0.511404 ± 14	−8.66 ± 0.28
JR8	Sweden/NAT	-	5.683	24.18	0.14211	0.511275 ± 25	−11.70 ± 0.50
IB1	U.S.S.R./NAT	0.70919 ± 4	75.00	346.9	0.13079	0.511372 ± 34	−9.28 ± 0.67
IB6	U.S.S.R./NAT	0.70924 ± 3	82.29	378.1	0.13165	0.511384 ± 11	−9.04 ± 0.22
IB7	U.S.S.R./NAT	0.70933 ± 3	59.05	268.5	0.13304	0.511357 ± 20	−9.58 ± 0.39
II. North American (except Southeastern U.S.)							
IB3	New York/C	0.70928 ± 7	214.2	636.1	0.20363	0.511544 ± 34	−5.91 ± 0.67
IB11	New York/MC	0.70835 ± 3	1.192	7.240	0.09958	0.510705 ± 41	−22.32 ± 0.81
C14	Oklahoma/MC	-	40.04	191.5	0.12643	0.510634 ± 12	−23.70 ± 0.24
IB22	Nevada/MC	-	0.683	4.347	0.09507	0.510905 ± 12	−18.51 ± 0.23
IB8	N.B., Canada/MV	0.70921 ± 5	216.8	945.5	0.13868	0.511053 ± 22	−15.52 ± 0.43
IB12	Nevada/MC	-	39.54	219.9	0.10876	0.510872 ± 24	−19.04 ± 0.46
IB2	Wisconsin/MC	0.70943 ± 8	209.3	961.2	0.13171	0.510618 ± 25	−24.02 ± 0.48
IB5	Wisconsin/MC	0.70963 ± 3	129.9	611.3	0.12847	0.510878 ± 13	−18.93 ± 0.25
IB10	Nevada/MC	-	66.21	332.9	0.12028	0.511032 ± 18	−15.92 ± 0.37
IB9	Nevada/MC	-	80.60	376.0	0.12968	0.511112 ± 20	−14.35 ± 0.40
III. Southeastern United States							
JR5a	Tennessee/MC	-	25.15	105.8	0.14382	0.511223 ± 39	−12.19 ± 0.80
JR5b	Tennessee/NAT	-	7.637	40.40	0.11436	0.511181 ± 20	−13.02 ± 0.40
IB4	Texas/MV	0.70939 ± 2	193.0	868.8	0.13439	0.511385 ± 19	−9.03 ± 0.38

[a] Fauna types: C, NAT, MC, MV are Cosmopolitan, North Atlantic, Mid-Continent, Mixed or Variable.

[b] Data normalized to $^{86}Sr/^{88}Sr = 0.1194$. The $^{87}Sr/^{86}Sr$ of NBS-987 was 0.71025 ± 2 and seawater was 0.70917 ± 2. Reported errors are 2σ of the mean.

[c] Uncertainty is 0.1%.

[d] Data normalized to $^{146}Nd/^{142}Nd = 0.636151$. The Caltech Nd standard nNdβ [28] gave $^{143}Nd/^{144}Nd = 0.511130 \pm 10$ and BCR-1 gave 0.511857 ± 15. Reported errors are 2σ of the mean.

[e] Deviations in parts in 10^4 from the present day bulk Earth (CHUR) value of $^{143}Nd/^{144}Nd = 0.511847$ [29].

in the Ordovician, our characterization of the Lower Paleozoic faunal provinces is oriented in terms of Ordovician faunal province names. In Table 2 and Fig. 1, the samples are also grouped according to their faunal affiliation: Mid-Continent (MC), North Atlantic (NAT), Mixed or Variable (MV) or Cosmopolitan (C).

The Ordovician "Mid-Continent" faunal province (MC) of conodonts corresponds closely to the "Pacific" or "North American" province of trilobites and brachiopods and is found mainly in North America. The conodont "North Atlantic" province (NAT), or corresponding "Acadio-Baltic" province of trilobites and brachiopods, has been found mainly in present-day Europe. The NAT province also occurs as a partial ring around the North American craton in deep-water facies. Acadio-Baltic trilobites have also been found in deep-water facies of easternmost and western North America. Mixed or Variable (MV) faunas are exemplified by the Middle Ordovician mixed brachiopod fauna facies along the eastern seaboard [20], and at other locations. The Silurian faunas are designated Cosmopolitan (C).

Our MC samples are all from North America. They are from northeast, southeast, midwest and western North American locations. All of our NAT fauna samples are from Europe, except one sample from Tennessee. MV and C faunal samples are from Europe and North America. North American MV sample locations are New Brunswick and Texas. The New Brunswick sample (IB12) is from the Gander terrane, described by Williams and Hatcher [25] as neither from cratonic North America nor Europe but from somewhere between the two. The Texan sample (IB5) is from

the southeastern edge of the Llano uplift. This is an area of periodic transgressive incursions of Atlantic fauna into a dominantly Pacific faunal sequence [26] and it is therefore considered variable.

4. Sample preparation and analytical techniques

Samples JR5a, JR5b, JR8 and C14 were separated from their carbonate rock matrix by dissolution of the carbonate with acetic acid. Samples IB9 and IB12 were separated from their rock matrix with formic acid. The phosphate fraction of these samples was separated from the rest of the residue by heavy liquids. All other samples were handpicked in our laboratory from the rock matrix using stainless steel microtools. All samples were rinsed repeatedly with ultrapure water prior to dissolution, weighed (1–10 mg per sample) and dissolved in $\approx 2N$ HCl acid. Next, samples were centrifuged to remove a small fraction of insoluble residue. The dissolved fraction was used for isotopic analysis. Mass spectrometric and chemical separation procedures for Sm-Nd and Rb-Sr follow the standard methods used at Harvard University [27]. Total processing blanks on Sr and Nd are 0.1–0.2 ng and 20–30 pg, respectively.

5. Results

Sm-Nd concentrations and isotopic results, and $^{87}Sr/^{86}Sr$ isotopic results are given in Table 2. In Fig. 2, measured $^{87}Sr/^{86}Sr$ ratios are plotted and compared to the curve of Burke et al. [4]. This curve provides a narrow range for the Sr isotopic composition of seawater during Phanerozoic times based on $^{87}Sr/^{86}Sr$ analyses of marine carbonates. Our samples plot on or close to this curve except for one sample from the beginning of the Silurian, a time during which this curve has no data points. It is possible to infer a sharp peak in the $^{87}Sr/^{86}Sr$ curve at this time both from this sample and from the Burke et al. [4] data. Although the Rb/Sr ratio was not measured for these samples, we measured very low Rb/Sr ratios of 0.0001 or lower for other samples of similar material, suggesting that corrections for decay of ^{87}Rb are negligible for these samples. The generally good agreement between the Burke et al. curve and our Sr isotope data suggests that the phosphatic fossil values actually

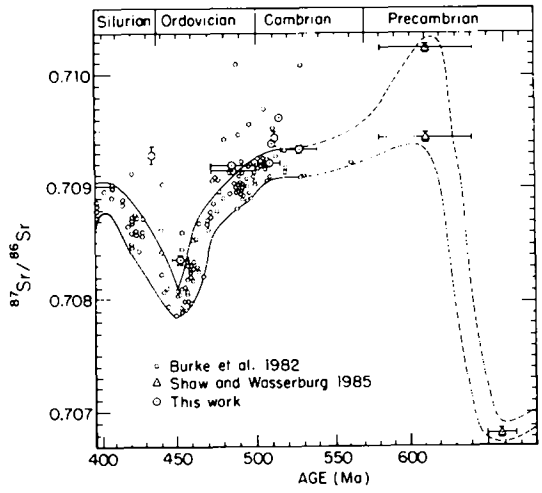

Fig. 2. The isotopic evolution of Sr in the oceans from the Late Precambrian through the Silurian. This figure includes our data, data from Burke et al. [4] and data from Shaw and Wasserburg [11]. The data of Burke et al. [4] are limestone and dolomite samples and the three points of Shaw and Wasserburg [11] are phosphorites. Our data are phosphatic fossils. In this figure, data from other laboratories has been corrected to be consistent with our measured value of $^{87}Sr/^{86}Sr$ in present-day seawater of 0.70917. The band enclosed by the solid line is that of Burke et al. [4]. We have dashed the curve for the Late Precambrian using the data of Shaw and Wasserburg [11].

represent, or are very close to, seawater isotopic values.

The $f_{Sm/Nd}$, initial ϵ_{Nd} and model ages for all samples are listed in order of increasing stratigraphic age in Table 3. Initial ϵ_{Nd} values were calculated with the stratigraphic ages (T_{STRAT}) using the Van Eysinga [18] time scale. Errors given for ages reflect relative uncertainties of the stratigraphic ages within the Van Eysinga time scale. Total absolute uncertainty in ages is somewhat larger and varies according to the age uncertainties of the tie-points of the time scale.

Most samples have $f_{Sm/Nd}$ values close to their mean value (-0.34), however, the range of variation is between $+0.03$ and -0.51. Single stage model ages relative to a depleted mantle (DM) evolution can be calculated using the CHUR values of Jacobsen and Wasserburg [29] together with $\epsilon_{Nd}(0) = +10$ for the modern value of the depleted mantle. This yields present-day values of $^{143}Nd/^{144}Nd = 0.512359$ and $^{147}Sm/^{144}Nd = 0.2136$ for the depleted mantle assuming a linear evolution of ϵ_{Nd} from $\epsilon_{Nd} = 0$ at the origin of the

TABLE 3

Initial Nd and model ages for biophosphate samples

Sample	T_{STRAT} [a]	$f_{Sm/Nd}$ [b]	T_{DM}^{Nd} (Ga) [c]	T_{2DM}^{Nd} (Ga) [c]	$\epsilon_{Nd}(T)$ location group [d]		
					EU	SE	NA
IB26	413 ± 1	−0.2804	2.02	1.62	−5.8 ± 0.3	–	–
IB3	432 ± 2	+0.0352	12.0	1.64	–	–	−6.3 ± 0.7
IB11	450 ± 5	−0.4937	2.20	2.54	–	–	−16.8 ± 0.9
JR5a	452 ± 3	−0.2688	2.48	1.93	–	−9.1 ± 0.8	–
C14	458 ± 7	−0.3572	3.01	2.79	–	–	−19.6 ± 0.3
JR8	460 ± 3	−0.2775	2.31	1.84	−8.0 ± 0.5	–	–
JR5b	463 ± 2	−0.4186	1.81	1.86	–	−8.1 ± 0.4	–
IB1	485 ±15	−0.3351	1.81	1.63	−5.2 ± 0.8	–	–
IB6	485 ±15	−0.3307	1.89	1.69	−5.0 ± 0.3	–	–
IB22	493 ± 7	−0.5167	1.87	2.20	–	–	−12.1 ± 0.4
IB8	508 ± 7	−0.2950	2.64	2.17	–	–	−11.8 ± 0.5
IB12	510.5 ± 0.5	−0.4471	2.15	2.31	–	–	−13.3 ± 0.5
IB4	511 ± 1	−0.3168	1.87	1.64	–	−4.9 ± 0.4	–
IB2	512 ± 2	−0.3304	3.22	2.83	–	–	−19.8 ± 0.5
IB5	513 ± 2	−0.3469	2.64	2.41	–	–	−14.5 ± 0.3
IB7	528 ±12	−0.3236	1.89	1.68	−5.3 ± 0.5	–	–
IB10	528 ± 3	−0.3885	2.17	2.13	–	–	−10.7 ± 0.4
IB9	560 ± 5	−0.3407	2.26	2.05	–	–	−9.6 ± 0.4

[a] Ages from Van Eysinga [18].

[b] $f_{Sm/Nd} = [(^{147}Sm/^{144}Nd)_{sample}/(^{147}Sm/^{144}Nd)^{0}_{CHUR}] - 1$ where $(^{147}Sm/^{144}Nd)^{0}_{CHUR} = 0.1967$ [29].

[c] Calculated using present-day depleted mantle values of $(^{143}Nd/^{144}Nd)_{DM} = 0.512359$ and $(^{147}Sm/^{144}Nd)_{DM} = 0.2136$.

[d] $\epsilon_{Nd}(T) = \{[(^{143}Nd/^{144}Nd)(T)_{sample}/(^{143}Nd/^{144}Nd)(T)_{CHUR}] - 1\} \times 10^{4}$ using CHUR values of [29].

Earth (see footnote in Table 3). Model ages calculated relative to such a DM reservoir are given by $T_{DM}^{Nd} = (1/\lambda_{Sm})\ln\{1 + [(^{143}Nd/^{144}Nd)_{meas} - 0.512359]/[(^{147}Sm/^{144}Nd)_{meas} - 0.2136]\}$ where $\lambda_{Sm} = 6.54 \times 10^{-12}\ a^{-1}$ (cf. Goldstein et al. [30]). The T_{DM}^{Nd} model ages for the EU samples range from 1.8 to 2.3 Ga; SE sample model ages are close to these values (1.8–2.5 Ga). Model ages for NA samples vary widely from 1.9 to 3.2 Ga. The oldest values are from samples located close to the center of the North American continent. One sample (IB3) has a 12 Ga model age which is due to its positive $f_{Sm/Nd}$ value. Other samples also have $f_{Sm/Nd}$ values that are somewhat higher than the

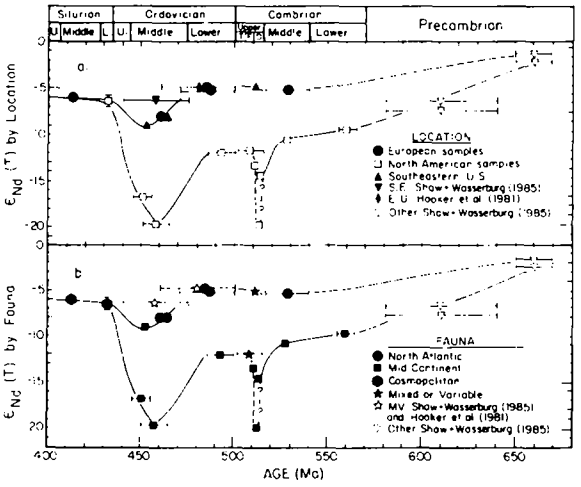

Fig. 3. The isotopic evolution of Nd in the oceans from the Late Precambrian through the Silurian. (a) ϵ_{Nd} is plotted as a function of time and location groups: Europe, North America and Southeastern United States. (b) ϵ_{Nd} is plotted as a function of time and faunal groups which are North Atlantic, Mid-Continent, Cosmopolitan and Mixed or Variable. Also shown is one sample of Hooker et al. [19] and five samples of Shaw and Wasserburg [11]. This represents all of the available data on ϵ_{Nd} of the oceans from 400 to 700 Ma. Two data trends are identified in both (a) and (b). The curve with ϵ_{Nd} of −5 to −9 represents the Iapetus Ocean as we have redefined it in the text. The curve with ϵ_{Nd} of −10 to −20 represents data of the Panthalassa Ocean. The two curves join in approximately the Late Ordovician, coincident with the Taconic Orogeny. Note that the ϵ_{Nd} trends appear to correlate more directly with sample location than with fauna.

typical continental value of -0.4 [30] suggesting fractionation in Sm/Nd relative to their continental sources. Thus, a two-stage model age is more appropriate for estimating the mean ages of the continental sources of Nd in our phosphate samples. We will discuss two-stage model ages in a later section.

Our Nd isotopic results are shown in an $\epsilon_{Nd}(T)$ versus age diagram in Fig. 3. Together with six previously published data points [11,19] plotted in this figure, these data represent all of the presently available data on the Nd isotopic composition of the oceans from 700 Ma to 400 Ma. Table 3 also groups the $\epsilon_{Nd}(T)$ results according to present geographic location and age. The groups are Southeastern North America (SE), the rest of North America (NA) and Europe (EU). NA is comprised of samples from both western (W-NA) and northeastern (NE-NA) North America. Table 3 shows that all EU samples from the Middle Cambrian through the Early Ordovician have uniform $\epsilon_{Nd}(T)$ within a range of -5.2 ± 0.8. The only SE sample measured for this interval has $\epsilon_{Nd}(T)$ identical to the EU samples. Middle Ordovician samples of EU and SE have $\epsilon_{Nd}(T)$ values of -8.0 to -9.1. The NA samples from the Lower Cambrian to the Middle Ordovician have consistently lower $\epsilon_{Nd}(T)$ values, ranging from -10 to -20. One Upper Cambrian NA sample has $\epsilon_{Nd}(T)$ of -19.8. This sample is from a site of maximum transgression of the Upper Cambrian seas onto the Archean of the Laurentian highlands of the North American interior [31]. Such low values seem quite limited in either space or time since another sample of nearly the same age from a location 50 miles away has $\epsilon_{Nd}(T)$ of -14.5. In general, samples of Late Cambrian age from North America, including both NE-NA and W-NA, have similar $\epsilon_{Nd}(T)$. Silurian samples from both EU and NA have $\epsilon_{Nd}(T)$ ratios of -5.8 and -6.3, respectively, identical within error.

In Fig. 3b, the $\epsilon_{Nd}(T)$ results are grouped according to the faunal affiliations of Mid-Continent (MC), North Atlantic (NAT), Mixed or Variable (MV), and Cosmopolitan (C). All MC fauna samples are found in North America, and have $\epsilon_{Nd}(T)$ of -9 to -16 or lower. All NAT fauna samples except one are from Europe and have higher $\epsilon_{Nd}(T)$ than MC samples. One NAT fauna sample from Tennessee has the same value within error to the essentially contemporaneous MC fauna sample from Tennessee. Sample of MV faunas have either MC or NAT $\epsilon_{Nd}(T)$ signatures rather than intermediate values. Silurian C faunas from both Europe and North America have identical $\epsilon_{Nd}(T)$ within error.

Overall, Fig. 3 shows two distinct trends in the $\epsilon_{Nd}(T)$ data. A comparison of the location distribution of the data in Fig. 3a with the faunal distribution patterns of Fig. 3b shows a strong similarity. However, the characterization of the data by location clearly separates in agreement with trends in $\epsilon_{Nd}(T)$ whereas there is some complication in the pattern of $\epsilon_{Nd}(T)$ according to faunal distributions. During the Late Cambrian to Middle Ordovician the NE-NA and W-NA samples have values that are very similar to each other, but the SE sample have values that are very different from the rest of NA and similar to EU regardless of faunal affinity. The simplest interpretation of the data is that the $\epsilon_{Nd}(T)$ trends represent two geographically distinct ocean water masses in the area between Paleozoic NA and Baltica. One of these water masses seems to have circulated freely from western NA to northeastern NA. The other water mass circulated between SE and EU. This interpretation contrasts with previous interpretations of ocean distributions in the Paleozoic. In particular, it diverges from the classical interpretation of one homogeneous Iapetus Ocean stretching between eastern Paleozoic North America and Baltica.

6. Discussion

6.1. Iapetus Ocean paleoceanography

In Wilson's historic 1966 paper, "Did the Atlantic close and then reopen?" [32], he referred to an ocean that was the precursor to the Atlantic, the Proto-Atlantic Ocean (later called Iapetus (cf. [33])). His original conclusions were based in part on faunal distributions. Since Wilson's paper, research on the Appalachian/Caledonian mountain chain has established that an ocean was present between North America and Baltica in the Early Paleozoic, and that this ocean closed during the Taconic/Caledonian and Acadian orogenies [33]. The present-day Atlantic Ocean began to open in the Jurassic, slightly to the east of the former suture between North America and Baltica [34,35].

Some Early Paleozoic reconstructions, such as Scotese et al. [36] show essentially one global ocean. If the Iapetus was a well-mixed ocean between North America and Baltica, then the ϵ_{Nd} data would have the same values at any time on all shores. However, our Cambrian/Ordovician samples from clearly autochthonous continental sequences in eastern North America have different ϵ_{Nd} values in the north and in the south. Also, there are different ϵ_{Nd} values between northeastern North America and Baltica until at least the Middle Ordovician. Therefore, there must have been two ocean water masses present in the area traditionally assigned to the Iapetus Ocean. Consequently, there must have been some barrier to circulation within the region formerly ascribed to the Iapetus Ocean, although the circulation barrier within this region did not last later than the Middle Ordovician. A dramatic shift in the ϵ_{Nd} value of the North American samples in the later Ordovician or earliest Silurian to values identical to those of European samples indicates unrestricted circulation between areas that previously had separate circulation, and is coincident with both the Taconic Orogeny of North America and the quick diminution of faunal provincialism. Apparently, the closing of Iapetus marks the formation of a globally well-mixed ocean.

The Cambrian to Middle Ordovician circulation barrier may have been an actual mechanical barrier to circulation, such as a chain of islands or continental fragments (causing lateral separation of water masses) or a physical/chemical barrier to circulation such as stratification of water masses. The circulation geometry of these two hypothetical distributions of Cambrian/Ordovician water masses is shown in Fig. 4.

The geometry of circulation in the case of a mechanical barrier is straightforward (Fig. 4a); essentially, there are two oceans within the area traditionally assigned to the Iapetus Ocean. Highlands within the Iapetus have been around under the names "geanticline" or "tectonic lands" since well before the adoption of plate tectonics by the geological community [37,38]. Recently, the Celtic terrane of brachiopods was identified as a chain of islands within the Iapetus [39]. Although it is recognized that the Iapetus was a complex and cluttered ocean [25,40,41], it has not previously been proposed that islands and shoal prevented

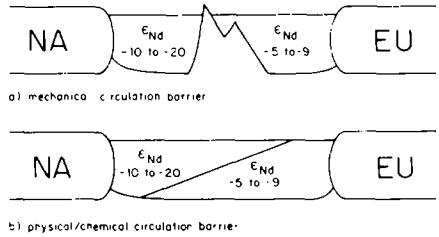

Fig. 4. Early Paleozoic schematic paleoceanography. (a) Mechanical circulation barrier. This figure depicts a model whereby northeastern North America and Europe (Baltica) are separated by two separately circulating ocean basins due to a barrier of an island or shoal chain. (b) Physical/chemical circulation barrier. This figure illustrates an alternate hypothesis whereby the two seawater masses between northeastern North America and Europe are stratified, due to poor circulation, polar gyres, or other causes. As discussed in the text, the Nd isotopic data are most consistent with (a).

circulation between a "northern" and "southern" ocean in the area of the Iapetus.

Another possible cause of the ϵ_{Nd} variations is stratification within the Iapetus Ocean. Stratification of ocean water or very slow overturn circulation has been suggested for various times in the Earth's history, including the Ordovician [14,22]. Fig. 4b shows one ocean circulation geometry for stratification. This model is consistent with conodont faunal distributions [22] and implies one wedge-shaped (cold) water mass that existed at all depths in the water column at high latitudes near Europe, but only at greater depths at low latitudes toward North America. Another water-wedge overrides the cold mass at low latitudes near North America, and pinches out at shallower and shallower depths with increasing latitude. A similar example today is Antarctic Deep Water that is exposed at the surface at high southern latitudes in the present day Atlantic Ocean and becomes deeper as it is traced northward [42].

From ϵ_{Nd} data of the EU and NA group samples, either hypothesis shown in Fig. 4 is possible. However, in Southeastern U.S., NAT and MC fauna occur in facies characteristic of very different depths of deposition, yet very close to each other with no apparent barrier. This faunal distribution indicates that either the faunal distribution is not strictly correlated to water mass or the water masses are not separated by a physical barrier.

In testing these alternate hypotheses, we chose Lower/Middle Ordovician samples from Tennes-

see that lie directly across the Saltville Fault. The Saltville Thrust Fault does not have very great lateral displacements, but has juxtaposed shallow and deep water facies. Across the fault lie separate provincial and endemic trilobites, brachiopods and conodonts [20]. Early Middle Ordovician age was chosen for the test because of the strong provincialism during this period, and because EU and NE-NA samples of this age have quite different ϵ_{Nd}. The sample JR5a is from west of the Saltville Fault in the Tazewell Confacies. JR5a is composed exclusively of MC fauna conodonts of the *Nemagraptus gracilis* Graptolite Zone. Sample JR5b is from east of the Saltville Fault in the Blount Confacies Belt. This sample is composed exclusively of NAT fauna conodonts with the very similar age of the *Glyptograptus teretiusculus* Graptolite Zone.

We may consider three different cases depending on the Nd isotopic results of these samples. First, if both samples have $\epsilon_{Nd}(T)$ signatures identical to other coeval MC fauna, a mechanical barrier was present through the length of the Appalachians. In this case, Iapetus would have exhibited vertical circulation within each of its two basins, but not lateral circulation across the whole ocean. Second, if both samples have distinctly different $\epsilon_{Nd}(T)$ signatures, there would have been restricted vertical circulation and stratification of water masses in the Iapetus region. A mechanical circulation barrier would not have been required. Finally, if both samples have $\epsilon_{Nd}(T)$ similar to coeval NAT fauna, circulation in Iapetus was not restricted vertically and stratification would not have existed in Iapetus. However, in order to explain the divergence of $\epsilon_{Nd}(T)$ signatures of faunas further north in the Appalachians, a mechanical barrier to circulation must have existed and two distinct ocean basins would have been required in this area.

In fact, the Tennessee MC sample, the Tennessee NAT sample and the coeval Swedish NAT sample have $\epsilon_{Nd}(T)$ values within error of each other. However, their $\epsilon_{Nd}(T)$ values are quite different from the Pennsylvania MC sample. This result is only consistent with the final case. Apparently, there was vertical circulation within Iapetus and a mechanical barrier to lateral circulation must have been present in the northern Appalachian region (which ended south of Pennsylvania and north of Tennessee).

We conclude that the Cambrian to Middle Ordovician Iapetus Ocean, classically refered to in the literature as existing between Paleozoic North America and Europe, was not a single homogeneous ocean. From the patterns shown by the ϵ_{Nd}, time, fauna and location data, different areas of the Iapetus Ocean had distinct ϵ_{Nd} signatures until at least the Middle Ordovician. The clearest, most simple interpretation of the ϵ_{Nd} distribution is that the NA samples and EU-SE samples represent isotopic ratios of two different ocean water masses from at least the Middle Cambrian to the Middle Ordovician; and represent one ocean water mass thereafter, beginning in the Late Ordovician or Early Silurian. Thus, we have identified two parts of the classical Iapetus Ocean; a "Southern Iapetus Sea" and a "Northern Iapetus Sea" which circulated separately until at least the Middle Ordovician. Clearly, tectonic events may be reflected in ϵ_{Nd} seawater values. The correspondence of the Taconic Orogeny tectonic event to a major $\epsilon_{Nd}(T)$ oceanic shift, points to the possibility that $\epsilon_{Nd}(T)$ seawater signatures may be used to help understand the tectonic history as well as the paleogeography of mountain belts.

6.2. Nd isotopic constraints on Ordovician paleogeography

In this section, we try to determine which existing paleogeographic maps are most compatible with the Nd isotopic data, and how they can be used to identify the size and location of the "Southern" and "Northern" Iapetus Seas and their relationship to the remaining world oceans in the Ordovician. Fig. 5a and b show simplified versions of two published paleogeographic maps from Ronov et al. [43] and Smith et al. [44], respectively. These maps are generally representative of the variations among the published Early Paleozoic paleogeographies [35,43–45]. The paleogeographic maps generally show one open and well-mixed global ocean during the Early Paleozoic, except for the map of Smith et al. [44], which depicts two oceans in the Early Paleozoic. Since the Nd isotopic data demand at least two different water masses until the Middle Ordovician or later, a first impression would indicate that Smith et al. [44] were more correct in the paleogeographic reconstruction.

The Ronov et al. [43] map in Fig. 5a is based on both geologic and paleomagnetic data, and is nearly identical to Bambach et al. [45] and Scotese et al. [35] in the distribution of continents and oceans. The Smith et al. [44] map in Fig. 5b relies only on paleomagnetic data. A significant difference between the paleogeographic reconstructions in 5a and b is the position of Baltica, labeled "BA" on these figures. According to Piper [46,47] there are no reliable paleomagnetic data for Baltica from the Cambrian to Early Ordovician, and Middle Ordovician paleopoles are inconsistent. Various paleogeographic interpretations have situated Baltica from 0 to 70° south latitude in the Early/Middle Ordovician. In Fig. 5a, Baltica is shown at high, southern latitude; in Fig. 5b it is nearly at the equator.

Fig. 5c and d, respectively, show the maps of 5a and b expanded to emphasize the areas around North America and Baltica. The sample location of the NA group (light stipple) and the SE-EU groups (dark stipple) are shown. An arrow to the south of North America represents restriction of circulation across this area. An arrow to the north of North America represents freedom of circulation in that region. A line of squares with x's are shown between Baltica and North America. These schematically represent our proposed island or shoal barrier. Approximate boundaries of exposed land areas in Europe and North America are also shown.

Both figures show the Cambrian to Middle Ordovician range in ϵ_{Nd} values for each ocean. The ocean that lies between North America and Baltica with ϵ_{Nd} of -5 to -8 is labeled Iapetus rather than the "Southern Iapetus Sea" as we

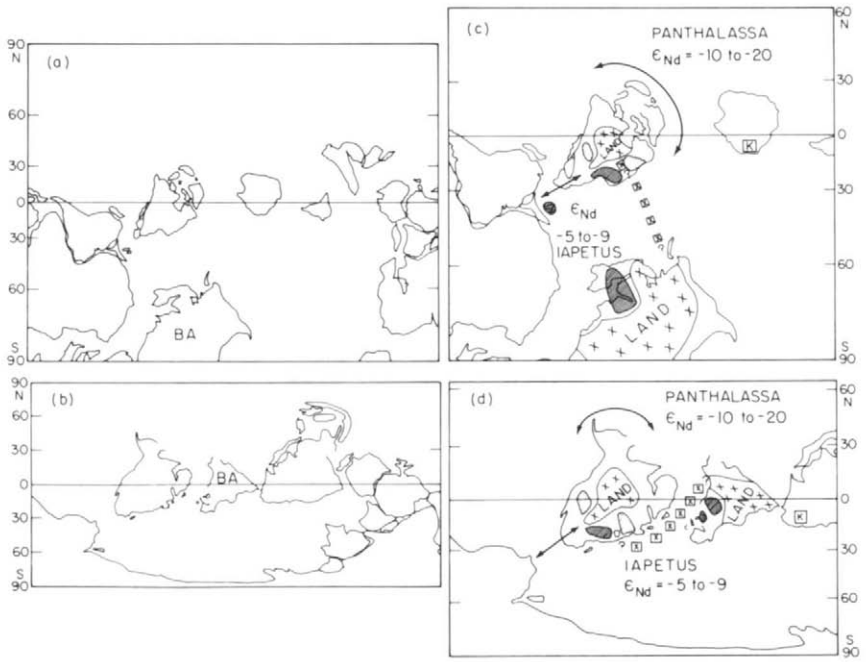

Fig. 5. Ordovician paleogeography. (a) Early Ordovician paleogeography, simplified from Ronov et al. [43]. This version is nearly identical to the Middle Ordovician paleogeography of Bambach et al. [45]. Both Ronov et al. [43] and Bambach et al. [45] rely on geologic as well as paleomagnetic data for the construction of their paleogeographic representations. (b) Middle Ordovician paleogeography, after Smith et al. [44]. This paleogeographic representation is constructed solely on the basis of paleomagnetic data. Although (a) and (b) are of slightly different times within the Ordovician, it is of no significance here. *BA* identifies the Baltica continent in (a) and (b). (c) and (d) show expansions of the (a) and (b) maps, respectively to emphasize the areas of North America, Baltica and the Iapetus Ocean in these figures. The sample location of the NA group (light stipple) and the SE + EU groups (dark stipple) are shown. A line of squares with x's is shown between Baltica and North America. These schematically represent our proposed island or shoal barrier to circulation. In (c) and (d) two oceans (Panthalassa and Iapetus) are shown together with their respective Cambrian/Ordovician range of ϵ_{Nd} values. Several lines of evidence (see text) including the ϵ_{Nd} value of -10.7 in the Kazakhstan sample (*K*) favor the paleogeography shown in (c).

called it earlier. The basis for assigning the name Iapetus to this region is that it is the predominant area in which the Proto-Atlantic Ocean of Wilson [32] was first defined. The other ocean with ϵ_{Nd} of -10 to -20 is referred to as Panthalassa rather than the "Northern Iapetus Sea". Historically, Panthalassa is considered the major ocean of the Late Paleozoic and Iapetus the major ocean of the Early Paleozoic. However, we have shown that the Iapetus was not a global ocean since the ϵ_{Nd} data clearly demonstrate the presence of two oceans in the early Paleozoic. Thus, the areas called Panthalassa and Iapetus in Figures 5c and 5d do not represent traditional locations, but our new interpretation of the extent of those oceans.

In Fig. 5c, the circulation barrier necessary to separate the different ϵ_{Nd} regions has a wide range of allowable geometric possibilities. In Fig. 5d, the island barrier is constrained to lie in a very narrow corridor to separate the waters of geographically close New York and Baltica, yet the barrier allows mixing of waters from Tennessee and Baltica which are geographically distant. Fig. 5c shows a much wider connection between the main body of Panthalassa and New York and New Brunswick than in the Fig. 5d paleogeometry. Since there are coherent trends in the ϵ_{Nd} data, it is probable that efficient circulation occurred between these areas and the main ocean. Therefore Fig. 5c with the widest connection, is the most appealing paleogeometry.

In addition, we have measured Nd isotopic ratios of inarticulate brachiopods from Kazakhstan, U.S.S.R. The sample came from the Batrybyr section in the Maly Karatua range ("K" in Fig. 5c and 5d). The age of this sample is of the lowermost *Hirsutodontus simplex* Conodont Subzone, and hence is from the base of the Ordovician period, defined as the base of the Tremadoc epoch. The Van Eysinga [18] age for this sample is 505.0 $\pm$ 0.5 Ma.

In the case of the reconstruction in Fig. 5d, this sample should be in the Iapetus Ocean and have an ϵ_{Nd} value close to -5; in the case of the reconstruction in Fig. 5c, the Kazakhstan sample should be in Panthalassa and have a lower ϵ_{Nd} value. In fact, the sample has $\epsilon_{Nd}(T)$ of -10.7 ($\epsilon_{Nd}(0) = -15.9$, $f_{Sm/Nd} = -0.389$) which is very close to Late Cambrian/Early Ordovician values of New Brunswick and Nevada, and unlike Late Cambrian/Early Ordovician values of Baltica and Texas. This indicates that the paleosouth part of Kazakhstan was affiliated with the Panthalassa rather than the Iapetus. Unless the paleopositioning of Kazakhstan is incorrect, this sample confirms that Fig. 5c is a more correct paleogeography than is Fig. 5d.

We conclude that the Early/Middle Ordovician paleogeographic reconstructions most compatible with ϵ_{Nd} data are those that position Baltica at high latitudes, and those in which Iapetus is a relatively small ocean as shown in Fig. 5c. Paleomagnetic data of this period for Baltica are limited. Original magnetic inclinations and declinations have not been obtained from Baltica samples of this age range because most stratified rocks of those ages were subject to thermal alterations and/or mechanical deformation in orogenic events. However, initial ϵ_{Nd} values can be obtained from rocks that did not preserve any particular orientation, and phosphatic samples preserve their ϵ_{Nd} signatures to approximately 350 °C. Hence, ϵ_{Nd} appears to be a useful tool extending and complementing paleomagnetic data in understanding paleogeographic relationships in orogenic areas.

6.3. Causes of conodont provincialism

The Early Cambrian through Middle Ordovician marked a period of increasing provincialism. Trilobites and brachiopods exhibited provincialism in the Cambrian whereas conodonts became provincial in the Early Ordovician. Provincialism was probably more extreme in the Middle Ordovician than at any other time in the Phanerozoic [20]. By the end of the Ordovician and into the Silurian, faunal provincialism waned and cosmopolitan fossils became the rule.

We can use the ϵ_{Nd} signature of faunas and faunal distribution to find causes for conodont faunal provinciality. A variety of factors characterize or determine whether biogeographically provincial or cosmopolitan faunas dominate at a particular time. Biogeographic provincialism indicates geographic distinctions among populations of fossils whereas cosmopolitan faunas are found in diverse locations or habitats. Generally, the geographic boundaries of faunal provinces are determined by some environmental distinction or barrer to migration. Biological discriminators of

environment can include sensitivity to water temperature, light availability, salinity, nutrient availability, and water depth or pressure. Patterns in the rock record of provincialism may be complicated by the habitation mode of faunas such as bottom dwelling, floating or swimming.

It has already been demonstrated that conodont provincialism is not determined by geographic isolation since different conodont faunas can occur in quite close association, as was the case in Tennessee. Nor is the cause depth sensitivity because conodont NAT faunas are found in shallow water facies near Baltica and in quite deep facies around North America. The ϵ_{Nd} pattern in Fig. 3b suggests that different faunas can be found in the same water mass. Therefore, conodonts do not seem to discriminate primarily on the basis of water mass characteristics such as nutrients or salinity. Water temperature can vary according to depth and latitude within one circulating water mass, such as in Antarctic Intermediate Water today [42]. Thus Sweet and Bergstrom's suggestion [22] that conodont provincialism is water-temperature dependent is not excluded by the pattern of ϵ_{Nd} data.

We suggest that in the Early and Middle Ordovician, periods of pronounced conodont provincialism, the temperature of shallow water near the Southeastern U.S. shore of the "Southern Iapetus Sea" was higher than the temperature of shallow water near the shore of Baltica. This temperature difference probably was due to a latitude gradient between the Baltica and Southern U.S. sides of the Southern Iapetus Sea. When Baltica moved closer to the equator during the closing of Iapetus (destruction of Northern Iapetus Sea), water temperature differences became smaller and faunal distinctions were minimized. Temperature seems to be the only environmental indicator that satisfies the paleogeographic pattern of ϵ_{Nd} and conodont faunas, as well as the timing of conodont provincialism.

6.4. Constraints on mean ages of Lower Paleozoic crust

The modern Pacific, Indian and Atlantic Oceans have average ϵ_{Nd} values of -3, -8, and -12 [1,2]. A typical continental $f_{Sm/Nd}$ value of -0.4 [30] yields T_{DM}^{Nd} model ages of 1.1 Ga, 1.5 Ga, and 1.8 Ga for the continental sources of Nd in each of these oceans. The rocks surrounding each ocean basin are dominated respectively by Paleozoic and younger rocks, mixed ages, and Proterozoic and older rocks [48]. Thus, variations in the $\epsilon_{Nd}(0)$ and T_{DM}^{Nd} model ages of seawaters to some extent reflect the mean ages of their continental source areas. The present day average ϵ_{Nd} value of seawater is -7 which yields a T_{DM}^{Nd} model age of 1.4 Ga [6].

The T_{DM}^{Nd} model age calculated from $\epsilon_{Nd}(0)$ of average seawater (using $f_{Sm/Nd} = -0.4$), need not be equal to the mean age of the continents, $\langle T \rangle$. First, it is possible that young crustal regions contribute proportionately more Nd to ocean water masses than is indicated by the "surface age distribution" of rocks in the drainage area for an ocean. Young orogenic areas erode faster, and hence put more sediment into the oceans than old stable areas [49]. This may yield suspended load model ages that are 0.2–0.4 Ga younger than the true mean age of the drainage area (Goldstein and Jacobsen, in preparation). Further, it is possible that ϵ_{Nd} in the dissolved load of many major rivers is 1–2 ϵ-units more radiogenic than the suspended loads of the same rivers [6]. This yields model ages for dissolved loads systematically 0.1–0.2 Ga younger than suspended load model ages. Thus, although T_{DM}^{Nd} model ages of the various oceans today clearly reflect the mean ages of their continental source areas, they may be systematically biased 0.3–0.6 Ga toward younger values. Assuming that this bias has not changed dramatically during the Phanerozoic, it should be possible to obtain an estimate of how $\langle T \rangle$ has changed since the Early Paleozoic.

Single-stage T_{DM}^{Nd} model ages were given in the results section. However, interpretation of model ages from ancient marine sedimentary minerals must be made carefully, because marine authigenic and biogenic phases often have $^{147}Sm/^{144}Nd$ ratios substantially different from their continental source rocks [11,14]. A two-stage model is necessary to represent mean continental model ages using model ages of fossil biophosphatic samples. The sample evolution from the time of deposition (T_{STRAT}) to the present is given by the $f_{Sm/Nd}$ value of the sample (f_{meas}); the sample evolution from the time of differentiation of the crustal source areas from the mantle to the time of deposition ($T_{2DM}^{Nd} - T_{STRAT}$) is given by the typical

continental crustal $f_{Sm/Nd}$ value of $f_{CC} = -0.4$ [30]. Thus, the two-stage model age (T^{Nd}_{2DM}) can be obtained from the single stage T^{Nd}_{DM} model age by the equation:

$$T^{Nd}_{2DM} = T^{Nd}_{DM} - \left(T^{Nd}_{DM} - T_{STRAT}\right)\left[\frac{f_{CC} - f_{meas}}{f_{CC} - f_{DM}}\right]$$

where $f_{DM} = 0.08592$ is the $f_{Sm/Nd}$ value of the DM reservoir.

The range in two-stage model ages (T^{Nd}_{2DM}) of Ordivician samples is 2.1–2.8 Ga for the NA group and 1.6–1.8 Ga for the EU + SE groups (Table 3). A rough mean age of crust exposed during the Early Paleozoic can be derived from these biophosphate model ages. The mean age is obtained by averaging the model ages within the NA and EU + SE groups of samples, and then averaging among the groups by weighting the groups by the size of the ocean water mass in which the samples are located. The average T_{STRAT} value of the samples is 490 Ma, or Early Ordovician age. Using the paleogeographic maps in Fig. 5c and d and assuming a similar average depth for the two ocean basins, the paleoceanic size of the Iapetus Ocean would have been between 0.05 and 0.20 of the size of the Panthalassa Ocean. The T^{Nd}_{2DM} averages of the NA group (Panthalassa) and SE + EU groups (Iapetus) are 2.3 Ga and 1.7 Ga. Using the estimated ocean sizes and their T^{Nd}_{2DM} values, an average T^{Nd}_{2DM} model age for the sources of Nd in Early Paleozoic oceans of approximately 2.2 Ga can be obtained. If the deposition age of 0.5 Ga is subtracted, the mean age estimate of the crust in the Early Ordovician was 1.7 Ga. This is similar to the mean age of approximately 1.8 Ga [50] for the crust today, and older than an analogous mean age estimated from the present-day oceans.

As shown by Jacobsen and Wasserburg [50], the rate of change of the mean age $\langle T \rangle$ is related to the continental mass (M) and its rate of growth ($dM/d\tau$) through the relationship $d\langle T \rangle/d\tau = 1 - (\langle T \rangle/M)(dM/d\tau)$ (assuming no recycling). Since the ocean data suggest that $\langle T \rangle = 1.4$ Ga today and 1.7 Ga at 0.5 Ga ago, we obtain $d\langle T \rangle/d\tau \approx -0.6$ for the last 0.5 Ga. It follows that the average rate of growth during this time must have been on the order of one crustal mass per Ga (i.e., $(dM/Md\tau) \approx 1\ Ga^{-1}$). Even considering the bias in the mean age estimates obtained using average seawater values, it appears difficult to totally change this result. This strongly suggests that substantial additions of new crust to the continents have continued throughout the Phanerozoic.

We conclude that the nature of the source terrane for the paleoceans is indicated by their ϵ_{Nd} signatures or Nd model ages. High ϵ_{Nd} values of -5 to -9 (representing the Iapetus Ocean) for EU and SE samples indicate substantial input from young orogenic, volcanic or island arc terranes, much like the present Pacific or Indian oceans. The very low ϵ_{Nd} values of -10 to -20 for the NA samples, shows the existence of very old crustal terranes that surrounded the Panthalassa Ocean in the Early Ordovician much like the present Atlantic Ocean. Most geologic research on this period has focussed on the active margins of the relatively small Iapetus Ocean rather than on the passive margins of the very large Panthalassa Ocean. The mean T^{Nd}_{2DM} model age of exposed crust in the Early Ordovician is about 1.7 Ga, similar to the mean age of the continental crust today.

Acknowledgements

We thank the curators of Harvard University's Museum of Comparative Zoology (all IB samples except IB9 and IB12), Bert Rowell of the University of Kansas (IB9, IB12), Tim Carr of ARCO Research (C14), John Repetski of the U.S. Geological Survey (JR5a, JR5b, and JR8) and Jim Miller of Southwestern Missouri State University (Kazakhstan sample) for providing samples. We thank Henry Shaw, John Repetski and an anonymous reviewer for helpful comments on the manuscript. This work was funded by NSF grants EAR 82-06954 and EAR 85-11912 to S.B.J.

References

1 D.J. Piepgras, G.J. Wasserburg and E.J. Dasch, The isotopic composition of neodymium in different ocean masses, Earth Planet. Sci. Lett. 45, 223–236, 1979.

2 D.J. Piepgras and G.J. Wasserburg, Neodymium isotopic variations in seawater, Earth Planet. Sci. Lett. 50, 128–138, 1980.

3 D.J. Piepgras and G.J. Wasserburg, Influence of the Mediterranean outflow on the isotopic composition of neodymium in waters of the North Atlantic, J. Geophys. Res. 88 C7, 5997–6006, 1983.

4 W.M. Burke, R.E. Denison, E.A. Hetherington, R.B. Koepnick, M.F. Nelson and J.B. Omo, Variations of seawater $^{87}Sr/^{86}Sr$ throughout Phanerozoic time, Geology 10, 516–519, 1982.

5 D.J. DePaolo and B.L. Ingram, High-resolution stratigraphy with strontium isotopes, Science 227, 938–941, 1985.

6 S.J. Goldstein and S.B. Jacobsen, The Nd and Sr isotope systematics of river water dissolved material: implications for the sources of Nd and Sr in seawater, Isot. Geosci., in press, 1987.

7 D.J. Piepgras and G.J. Wasserburg, Strontium and neodymium isotopes in hot springs on the East Pacific Rise and Guaymas Basin, Earth Planet. Sci. Lett. 72, 341–356, 1985.

8 E.T.C. Spooner, The strontium isotopic composition of seawater, and seawater-oceanic crust interaction, Earth Planet. Sci. Lett. 31, 167–174, 1976.

9 F. Albarède, A. Michard, J.F. Minster and G. Michard, $^{87}Sr/^{86}Sr$ ratios in hydrothermal waters and deposits from the East Pacific Rise at 21° N, Earth Planet. Sci. Lett. 55, 229–236, 1981.

10 L.S. Keto and S.B. Jacobsen, Implications for paleoceanography from Nd and Sr isotope ratios of Lower Paleozoic brachiopods, EOS Trans., Am. Geophys. Union 66, 424, 1985.

11 H.F. Shaw and G.J. Wasserburg, Sm-Nd in marine carbonates and phosphates: Implications for Nd isotopes in seawater and crustal ages, Geochim. Cosmochim. Acta 49, 503–518, 1985.

12 H. Staudigel, P. Doyle and A. Zindler, Sr and Nd isotope systematics in fish teeth, Earth Planet. Sci. Lett. 76, 45–56, 1985.

13 M.R. Palmer and H. Elderfield, Rare earth elements and neodymium isotopes in ferromanganese oxide coatings of Cenozoic foraminifera from the Atlantic Ocean, Geochim. Cosmochim. Acta 50, 409–417, 1986.

14 J. Wright, R.S. Seymour and H.F. Shaw, REE and Nd isotopes in conodont apatite; variations with geological age and depositional environment, in: Conodont Biofacies and Provincialism, D.L. Clark, ed., Geol. Soc. Am., Spec. Pap. 196, 325–340, 1984.

15 A.G. Epstein, J.P. Epstein and L.D. Harris, Conodont color alteration—an index to organic metamorphism, U.S. Geol Surv. Prof. Pap. 995, 1–27, 1977.

16 W.T. Holser, Gradual and abrupt shifts in ocean chemistry during Phanerozoic time, in: Patterns of Change in Earth Evolution, Dahlem Konferenzen, H.D. Holland, H.D. and A.F. Trendall, eds., pp. 124–143, Springer-Verlag, Berlin-Heidelberg-New York, 1984.

17 J. Wright, Rare earth element distribution in recent and fossil apatite: Implications for paleoceanography and stratigraphy, 259 pp., Ph.D. Dissertation, University of Oregon, 1985.

18 F.W.B. Van Eysinga, Geological Timetable, Elsevier, Amsterdam, 1975.

19 P.J. Hooker, P.J. Hamilton, and R.K. O'Nions, An estimate of the Nd isotopic composition of Iapetus seawater from Ca 490 Ma metalliferous sediments, Earth Planet. Sci. Lett. 56, 180–188, 1981.

20 V. Jaanusson, Ordovician, in: Treatise on Invertebrate Paleontology Part A: Introduction, Fossilization (Taphonomy), Biogeography and Biostratigraphy, R.A. Robison and C. Teichert, eds., pp. A136–A166, Geological Society of America, Boulder, Colo., and University of Kansas, Lawrence, Kans., 1979.

21 A.R. Palmer, Cambrian, in: Treatise on Invertebrate Paleontology Part A: Introduction, Fossilization (Taphonomy), Biogeography and Biostratigraphy, R.A. Robison and C. Teichert, eds., pp. A119–A135, Geological Society of America, Boulder, Colo., and University of Kansas, Lawrence, Kans., 1979.

22 W.C. Sweet and S.M. Bergstrom, Conodont provinces and biofacies of the Late Ordovician, in: Conodont Biofacies and Provincialism, D.L. Clark, ed., pp. 69–88, Geol. Soc. Am., Spec. Pap. 196, 1984.

23 A. Williams, Distribution of brachiopod assemblages in relation to Ordovician palaeogeography, in: Organisms and Continents Through Time, N.F. Hughes, ed, Spec. Pap. Paleontol. 12, 241–269, 1973.

24 G.M. Bennison and A.E. Wright, The Geological History of the British Isles, 406 pp., Edward Arnold, Ltd., London, 1969.

25 H. Williams and R.D. Hatcher, Jr., Appalachian suspect terranes, in: Contributions to the Tectonics and Geophysics of Mountain Chains, R.D. Hatcher, H. Williams and I. Zietz, eds., pp. 33–53, Geol. Soc. Am. Mem. 158, 1983.

26 C.H. Holland, Cambrian of the New World, 456 pp., John Wiley, New York, N.Y., 1971.

27 S.B. Jacobsen and R.F. Dymek, Nd- and Sr-isotope systematics of clastic metasediments from Isua, West Greenland: identification of pre-3.8 Ga old differentiated crustal components, J. Geophys. Res., in press, 1987.

28 G.J. Wasserburg, S.B. Jacobsen, D.J. DePaolo, M.T. McCulloch and T. Wen, Precise determinations of Sm/Nd ratios; Sm and Nd isotopic abundances in standard solutions, Geochim. Cosmochim. Acta 47, 2311–2323, 1981.

29 S.B. Jacobsen and G.J. Wasserburg, Sm-Nd isotopic evolution of chondrites and achondrites, II. Earth Planet. Sci. Lett. 67, 137–150, 1984.

30 S.L. Goldstein, R.K. O'Nions and P.J. Hamilton, A Sm-Nd isotopic study of atmospheric dusts and particulates from major river systems, Earth Planet. Sci. Lett. 70, 221–236, 1984.

31 Shell Oil Company, Stratigraphic Atlas, North and Central America, Shell Oil Company, Houston, Texas, 1975.

32 J.T. Wilson, Did the Atlantic close and then reopen?, Nature 211, 676–681, 1966.

33 J.D. Keppie, The Appalachian collage, in: The Caledonide Orogen—Scandinavia and Related Areas, D.G. Gee and B.A. Sturt, eds. pp. 1217–1226, John Wiley and Sons, New York, N.Y., 1985.

34 J. Rodgers, The Eastern Edge of the North American Continent during the Cambrian and Early Ordovician, in: Studies of Appalachian Geology: Northern and Maritime, E-An Zen, W.S. White, J.B. Hadley and J.B. Thompson, Jr., eds., pp. 141–150, John Wiley and Sons, New York, N.Y., 1968.

35 E.R. Deutsch, Mid-Ordovician paleomagnetism and the

Proto-Atlantic Ocean in Ireland, in: Plate Reconstructions From Paleozoic Paleomagnetism, R. Van der Voo, C.R. Scotese, and N. Bonhommet, eds., Am. Geophys. Union, Geodyn. Ser. 12, 116–119, 1984.

36 C.R. Scotese, R.K. Bambach, C. Barton, R. Van Der Voo and A.M. Ziegler, Paleozoic base maps, J. Geol. 87, 3, 217–277, 1979.

37 C. Schuchert, Sites and nature of the North American geosynclines, Geol. Soc. Am. Bull. 34, 151–229, 1923.

38 M. Kay, North American geosynclines, Geol. Soc. Am. Mem. 48, 143 pp., 1951.

39 D.L. Bruton and D.A.T. Harper, Early Ordovician (Arenig-Llanvirn) faunas from oceanic islands in the Appalachian Caledonide orogen, in: The Caledonide Orogen —Scandinavia and Related Areas, D.G. Gee and B.A. Sturt, eds., pp. 359–368, John Wiley and Sons, New York, N.Y., 1985.

40 J.F. Dewey, The evolution of the Appalachian Caledonian orogen, Nature 222, 124–129, 1969.

41 J.M. Bird and J.F. Dewey, Lithosphere plate-continental margin tectonics and the evolution of the Appalachian orogen, Geol. Soc. Am. Bull. 81, 1031–1060, 1970.

42 G.L. Pickard, Descriptive Physical Oceanography, 233 pp., Pergammon Press, Oxford, 1979.

43 A. Ronov, V. Khain and K. Seslavinsky, Atlas of Lithological-Paleogeographic Maps of the World, Late Precambrian and Paleozoic of Continents, USSR, 69 pp., Leningrad, 1984.

44 A.G. Smith, A.M. Hurley and J.C. Briden, Phanerozoic Paleocontinental World Maps, 101 pp., Cambridge University Press, Cambridge, England, 1981.

45 R.K. Bambach, C.R. Scotese and A.M. Ziegler, Before Pangea: The geographies of the Paleozoic world, Am. Sci. 8(1), 26–38, 1980.

46 J.D.A. Piper, Continental movements and breakup in Late Precambrian-Cambrian times: Prelude to Caledonian orogenesis, in: The Caledonide Orogen—Scandinavia and Related Areas, D.G. Gee and B.A. Sturt, eds., pp. 19–34, John Wiley and Sons, New York, N.Y., 1985.

47 J.D.A. Piper, Paleomagnetism in the Caledonian-Appalachian orogen: A review, in: The Caledonide Orogen—Scandinavia and Related Areas, D.G. Gee and B.A. Sturt, eds., pp. 35–53, John Wiley and Sons, New York, N.Y., 1985.

48 K.C. Condie, Plate Tectonics and Crustal Evolution, 310 pp., Pergamon Press, Oxford, 1982.

49 J.D. Milliman and R.H. Meade, World-wide delivery of river sediment to the oceans, J. Geol. 91, 1–21, 1983.

50 S.B. Jacobsen and G.J. Wasserburg, The mean age of mantle and crustal reservoirs, J. Geophys. Res. 84, 1001–1017, 1979.